PCCP

Accepted Manuscript

ROYAL SOCIETY OF CHEMISTRY

www.rsc.org/pccp

Anomalous high adsorption energy of H_2O on Fluorinated Graphenes: A First Principle Study

Peng Wang, Hongtao Wang, Wei Yang**

Institute of Applied Mechanics, Zhejiang University, Hangzhou 310027, China

ABSTRACT

Polytetrafluoroethylene (PTFE) has been well-known for the surface superhydrophobicity, while its two-dimensional stable analogues, CF and C_4F, possess distinct surface wettability. The CF inherits the hydrophobicity from PTFE since the *van der* Waals interaction is mitigated by the high electronegativity of fluorine. Surprisingly, high adsorption energy (~550 meV/molecule) of water has been unveiled on C_4F *via* density functional theory studies, implying anomalous superhydrophilicity of C_4F. The abrupt transition from hydrophobicity of CF to superhydrophilicity of C_4F can be reconciled with the difference in their molecular orbitals. The high adsorption energy of C_4F is mainly attributed to the Coulomb attraction among the non-bonding interactions, as proposed by our theoretical model. Since the surface chemical inertness of CF inhibits it from being widely adopted in device fabrication, the present finding suggests that C_4F can be a promising candidate in graphene-based electronic devices.

* To whom correspondence should be addressed. Email: htw@zju.edu.cn and yangw@zju.edu.cn

I. Introduction

Polytetrafluoroethylene (PTFE) has been well-known for the superhydrophobicity, due to the *van der* Waals forces mitigated by the high electronegativity of fluorine. Both the high strength of C-F bonds and the lack of unpaired electrons lead to extreme surface chemical inertness. Its two-dimensional analogue, fluorographene, since its synthesis in 2010, has attracted great attentions for applications in graphene-based electronics due to the presence of a wide band gap.[1-6] The similarity in structures renders fluorographene with similar chemical inertness to PTFE.[2, 7] However, its superhydrophobic surface inhibits it from being integrated with ultrathin high-κ dielectrics, as implemented in most device fabrications. Surface functionalizations may be a viable route, as adopted in graphene electronics, in order to comply with the widely used thin film deposition techniques, such as atomic layer deposition (ALD).[8-10]

A close observation reveals a large difference in electronegativity between F (3.98) and C (2.55). The high polarity of the C-F bonds may acquire significant attraction to small polar molecules, such as water or ammonia as co-reactants in ALD. For the bulk PTFE, the positively charged C atoms are all hidden beneath the surface F atoms, having less electrostatic attraction to the negative charge centers in adsorbates. Considering the two dimensional feature, one may tailor fluorinated graphenes (FG) to enhance the Coulomb interaction by varying the F/C ratio.

In this work, we systematically studied the water adsorption on fluorinated graphenes with three different F/C ratios by density functional theory (DFT)

simulations. High adsorption energy of water has been observed in C_4F (another stable fluorocarbon derivative of graphene with similar bandgap to fluorographene), implying anomalous superhydrophilicity of C_4F. This finding suggests that C_4F may replace CF as a promising candidate in graphene-based electronic devices, which provides an alternate route to resolve the key difficulty due to the surface chemical inertness.

II. Simulation

Adsorption energy, consisting of the *van der* Waals, electrostatics and induction interactions, is still a major challenge for the *ab initio* calculations. Though the widely used DFT provides excellent description of covalent and ionic bondings in condensed matters, it fails to reproduce accurately the above non-bonding interaction.[11, 12] Various methods have been developed, *e.g.* generalized gradient approximations (GGA), local density approximations (LDA), *van der* Waals density-functional (vdW-DF) and random-phase approximation (RPA). Among them, the RPA method considers all plasmon interactions and predicts the vdW interaction with the highest accuracy.[12, 13] However, its high computational cost discourages a systematic study on the adsorption in large systems. Recently, various vdW-DFT methods[11, 14] have been proposed in order to catch the long-range nature of vdW interaction by introducing a series of nonlocal correction functions. However, large discrepancies in adsorption energies remain among the calculations using different vdW-DFT methods.[11, 13, 14] In practice, both GGA and LDA methods are widely adopted for the estimation of non-bonding interactions. Though the adsorption energy by LDA is known to present

by freak occurrence rather than by conscious design, LDA method has been shown to be consistent with experiments in the case of graphene adsorption.[11] On balance of both accuracy and efficiency, we employed the LDA method in this research; meanwhile, used the GGA method as reference. The water-water interaction and entropic effect can hardly be considered in DFT simulations for the high computational cost. Nevertheless, the DFT simulations provide deep insight into the interactions, bearing the merit of less *ad hoc* hypothesis, which would pave the way for developing a well-suited force field for accurate MD simulations of the interaction between water molecules and FG substrates.

The first principle calculations were performed within the framework of DFT implemented in Quantum Espresso.[15] The ultra-soft pseudo-potentials of RRKJ type[16] were employed within the local density approximation (LDA) for the exchange-correlation potentials. The kinetic energy cutoff for the plane-wave basis set was taken to be 40 Ry. The self-consistency error was set to be less than 10^{-8} Ry. A Monkhorst-Pack[17] *k*-point mesh of 4×4×1 was used for the structural optimization and a denser Monkhorst-Pack grid of 16×16×1 was applied in calculating the density of states (DOS). The residual force components on each atom were set to be less than 10^{-3} eV/Bohr for the structural optimization. A vacuum space of ~20 Å was inserted between the consecutive slabs in order to nullify the interaction with periodic images.

The fluorinated graphenes have been successfully prepared by exposing graphene to the XeF_2 ambient.[1, 18] Nano fluorinated chains[19] and patches[5] have been observed in the products. The F/C ratios can be controlled in a large range by choosing proper

experimental conditions, such as temperatures and exposure time.[6, 18] However, limited by the characterization techniques, there is no clear evidence of the presence of C_4F or C_9F patches. In this work, fluorinated graphenes CF, C_4F and C_9F, for the high symmetries (Figure 1a,b,c)), were taken as model systems in order to study the F/C ratio effect on the stability and wettability of fluorinated graphenes. In all setups, the F atoms were located on both sides of graphene to form a chair configuration, which is known to be energetically favorable.[20, 21] The binding energies of an F atom are -2.90 eV, -2.85 eV and -2.04 eV for CF, C_4F and C_9F, respectively.

The water adsorption energy (E_a) is calculated as

$$E_a = E_t - E_g - E_w \quad (1)$$

where E_t, E_g and E_w represent the total energies of the H_2O/FG system, the isolated FG and the isolated H_2O molecule in the same supercell. Four different adsorption sites has been considered for CF, which are the center of the hexagonal ring (A), the top of a fluorine atom (B), the middle of the C-C bond (C) and the top of a carbon atom (D), as labeled in Figure 1a. For both C_4F and C_9F, more adsorption sites were considered (Figure 1b,c). For each site, we set up three possible orientations of the water molecule as the initial configurations (Figure 1d), *i.e.* one hydroxyl group pointing down to the fluorinated graphene (termed the "one-leg" position), both H atoms facing down (the "two-leg" position) and only O atom facing down (the "reverse" position). The total energy calculation is based on the full optimization of all atomic positions in the system.

Charge transfers are calculated based on the Löwdin population analysis, as

implemented in Quantum Espresso.[15] The atomic charge for each atom is obtained by the integration of electronic density of states projected onto orthogonalized atomic orbitals. The height of adsorbed H_2O molecule on FG basal plane is calculated as the distance between the lowest atom in H_2O and the neutral plane of FG.

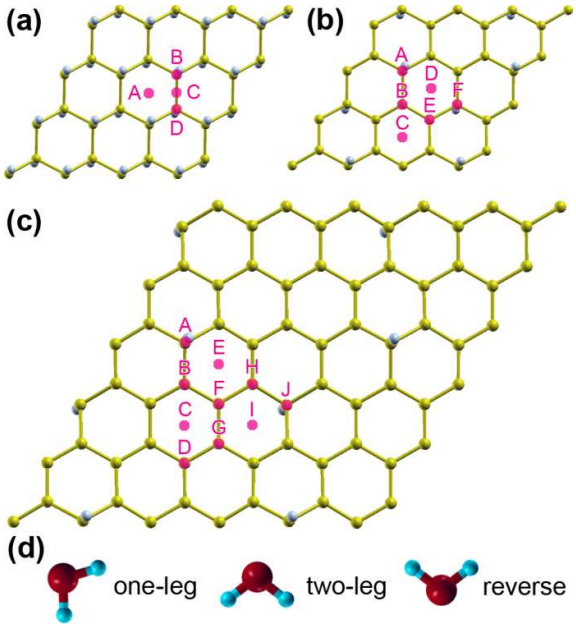

Figure 1. (a-c) The DFT optimized FG configurations marked with the selected high symmetry adsorption sites for CF, C_4F and C_9F, respectively; (d) The one-leg, two-leg and reverse orientations of water molecule in the initial setups.

III. Results

A. Water adsorption on CF surface

Table I lists the adsorption energies and the heights of H_2O molecules adsorbed on CF, showing the dependence of the adsorption energies on both the orientations and the adsorption sites. For CF, it is noted that the orientations of the water molecule slightly changed between the final configurations and the corresponding initial setups

(Figure S1). At each site, the adsorption energy was maximized only if H atoms got closer to CF, indicating the dominance of the dipole-dipole interaction between O-H and C-F. The most energetically favorable configuration (No. 1 in Table I) was attained when the hydroxyl group bi-sectioning two neighboring F atoms (Figure 2). The corresponding adsorption energy and the height of the adsorbed H_2O molecule are –117 meV and 3.24 Å, respectively. It is interesting to note that the water molecule on graphene has a lower adsorption energy (-151 meV).[22] This indicates the weak hydrogen bonding O-H···F and explains the slight change of the initial configuration during optimization.

TABLE I. Adsorption energies (E_a) and heights (d) of a H_2O molecule on CF at different sites and with different orientations.

No.	Position	Orientation	E_a (meV)	d (Å)
1[a]	A	one-leg	-117	3.24
2		two-leg	-94	3.66
3		reverse	-64	3.98
4	B	one-leg	-70	3.56
5		two-leg	-71	3.91
6		reverse	-48	4.24
7	C	one-leg	-84	3.45
8		two-leg	-88	3.70
9		reverse	-55	4.08

10	D	one-leg	-116	3.24
11		two-leg	-94	3.66
12		reverse	-65	3.99

[a]: The most energetically stable configuration

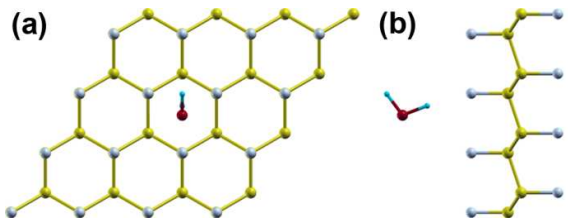

Figure 2. The top view (a) and side view (b) of the energetically favorable structure (No. 1) of a H_2O molecule on CF.

B. Water adsorption on C_4F surface

Much higher adsorption energies have been found in the H_2O/C_4F systems (Table II). The maximum adsorption energy is approximately -550 meV per water molecule. The final configuration, as shown in Figure 3a, has been attained with various initial setups (No. 22-27 and 29 in Table II). The two hydroxyl groups are aligned with the neighboring F atoms. Meanwhile, the oxygen atom is located directly on top of the sp^3-hybirdized C atom (O-C distance 2.66 Å) with the F atom on the other side. The high adsorption energy is due to the strong interaction between the negatively charged O atom and the positively charged C atom, which also explains the independence of the optimized configuration on the initial setups. Other infrequently observed configurations also show high affinity to the water molecule, as shown in Figure 3b,c,d. The four configurations can be classified into two basic types depending on

the locations of the oxygen atom. For the type I configurations (Figure 3a,b), the O atom is located on the position F in Figure 1b, which is characterized by the sp^3-hybridized C atom. The typical adsorption energy is about –500 meV per water molecule. The position C in Figure 1b is the second preferable adsorption site. Figure 3c and 3d show the secondary stable configuration with the O atom located on the position C (type II configuration). The typical adsorption energy is about -300 meV per water molecule. Among configurations of the same type, the small difference in adsorption energies is due to the specific orientation of the water molecule. It is noted that the positions B, D and E are not energetically favorable for water molecules, due to the strong attraction from the nearby sites C or F. At the position A, the O atom has a larger separation with sp^3 C and thus less interaction with C_4F.

TABLE II. Adsorption energies (E_a) and heights (d) of a H_2O molecule on C_4F at different sites and with different orientations.

No.	Position	Orientation	E_a (meV)	d (Å)
13	A	one-leg	-105	3.63
14		two-leg	-58	3.96
15		reverse	-11	4.56
16	B	one-leg	-134	3.35
17		two-leg	-549	2.37
18		reverse	-301	2.75
19	C	one-leg	-163	2.63

20		two-leg	-312	2.80
21		reverse	-300	2.73
22[a]	D	one-leg	-550	2.35
23[a]		two-leg	-549	2.38
24[a]		reverse	-550	2.38
25[a]	E	one-leg	-550	2.39
26[a]		two-leg	-550	2.39
27[a]		reverse	-549	2.40
28	F	one-leg	-166	2.54
29[a]		two-leg	-550	2.35
30		reverse	-468	2.35

[a]: The most energetically stable configuration

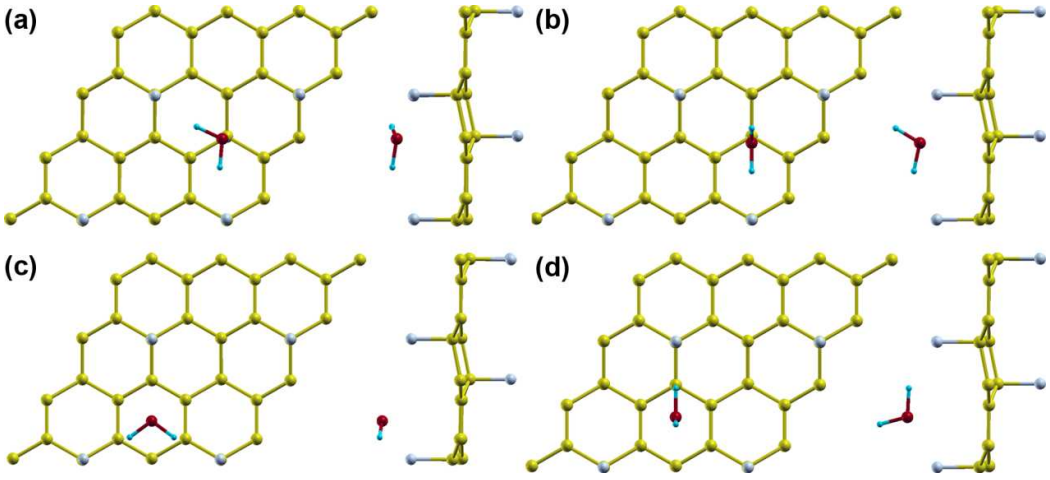

Figure 3. The top view (left) and side view (right) of the energetically favorable structures of a H_2O molecule on C_4F substrate: (a) No. 24, (b) No. 30, (c) No. 20 and (d) No. 18.

C. Water chemisorption on C_9F surface

When interacting with water molecules, less structural stability of the fluorinated graphene is caused by further lowering on the F/C ratio. DFT simulations show abnormally high adsorption energies above –2000 meV (Table III), indicating a chemisorption process. A typical result is shown in Figure 4. The energy minimization leads to reorientation of the water molecule and formation of a precursor state (Figure 4b). The C-F bond is elongated from 1.49 Å to 2.38 Å and weakened upon the approaching of the H atom. The chemical species HF is then released, leaving a free hydroxyl radical (Figure 4c). The reactive sites were identified to be three sp^2 C atoms neighboring to the sp^3 C atom with F atom on the opposite side. The covalent bonding of C-OH locally transforms the atomic hybridization from sp^2 to sp^3.

TABLE III. Chemisorption energies (E_a) of a H_2O molecule on C_9F at different sites and with different orientations.

No.	Position	Orientation	E_a (meV)
31	E	one-leg	-2687
32		reverse	-2014
33	F	one-leg	-2015
34		two-leg	-2690
35		reverse	-2687
36	G	two-leg	-2685
37	H	one-leg	-2024
38		two-leg	-2021

39		reverse	-2023
40	I	one-leg	-2023

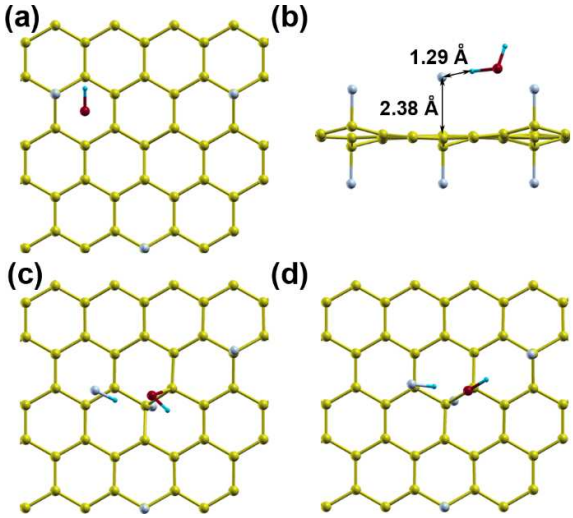

Figure 4. A typical chemisorption process of a H_2O adsorbed on C_9F. (a) The initial setup (No. 31); (b) Precursor state; (c) Release of HF; and (d) Formation of covalent bond C-OH.

The structural stability is closely related to the C-F bonding characters in CF, C_4F and C_9F, as shown in Figure 5a. The corresponding bond lengths are 1.36 Å (CF), 1.45 Å and 1.49 Å (C_9F), respectively, whilst the binding energies of the F atom are -2.90 eV, -2.85 eV and -2.04 eV (Figure 5b). This trend is consistent with the observed less structural stability in fluorinated graphenes with a lower F/C ratio.[1, 4, 18] Projected DOS analysis reveals that the charge transfer from C atom to F atom increases with a lowering F/C ratio (Figure 5b), indicating the transition from the covalent bonding in CF to the semi-ionic bonding in C_9F.[21] This is manifested by the decreasing of the charge density in the middle of the C-F bonds (Figure 5a). The partly ionic nature renders high reactivity of the C-F bonds in C_9F with water molecules.

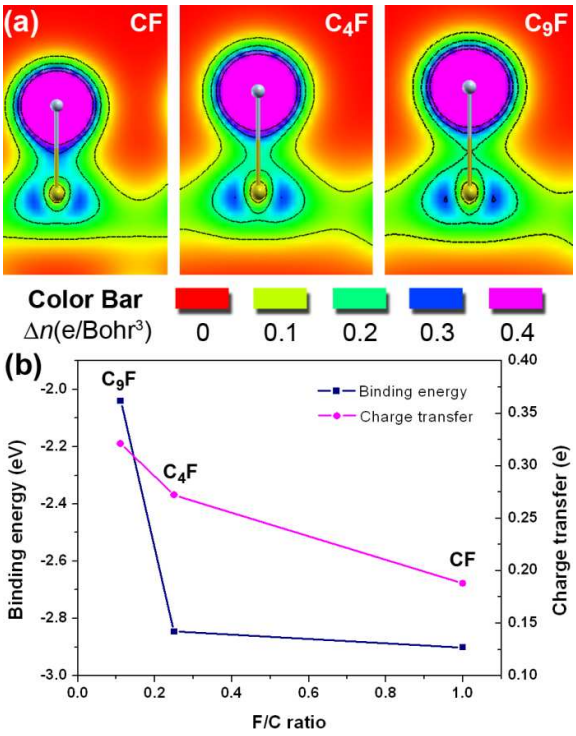

Figure 5. (a) Charge density contours of C-F bonds in CF, C_4F and C_9F; (b) Dependence of the binding energy and charge transfer of C-F bonds on the F/C ratio in fluorinated graphenes.

IV. Discussions

A. Orbital hybridization analysis

Figure 6 shows the charge distribution of water molecules on the fluorinated graphene. The physisorption nature is revealed by the low charge density between the adsorbates and the adsorbents in both systems. Further analysis shows substantial difference in the molecular orbitals between CF and C_4F (Figure 7). The valence band (VB) maximum and the conduction band (CB) minimum of CF and C_4F are depicted in the DOS plots. The bandgaps are 2.99 eV and 2.73 eV for CF and C_4F, respectively. For CF, the VB maximum is mainly located on F atoms and C-C bonds, while the CB minimum is distributed around the sp^3-hybridized C atoms (Figure 7b). On the other

hand, both the VB maximum and CB minimum in C_4F mainly surround the sp^2 hybridized C atoms, which bears similarities to those bands in graphene.[23] Only some VB maximum orbitals present around the F atoms. Since the highest occupied molecular orbitals (HOMO) of water molecules is located on the O atoms (inset to Figure 7a), a preferable adsorption configuration will align the O atom with C atoms in the fluorinated graphene to maximize the overlap of the interacting orbitals. Alignment of H atoms to F atoms can be realized by rotating the water molecule around the axis perpendicular to the surface and passing through the oxygen atom, leading to further orbital hybridizations. For CF, it is noted that the CB minimum is underneath the VB maximum, preventing the approach of O atom. A large separation between the O atom and C atoms renders the dominant role of the interaction between H and F atoms. This is also manifested by the charge transfer, scaled with the orbital hybridization. It is 0.043 e per water molecule for H atoms, but – 0.007 e for the O atom (Figure 6a). In contrast, the CB minimum of C_4F can be accessed by the HOMO of H_2O due to a lower F/C ratio, leading to a substantial increase of charge transfer for the O atom (– 0.037 e for Figure 6b).

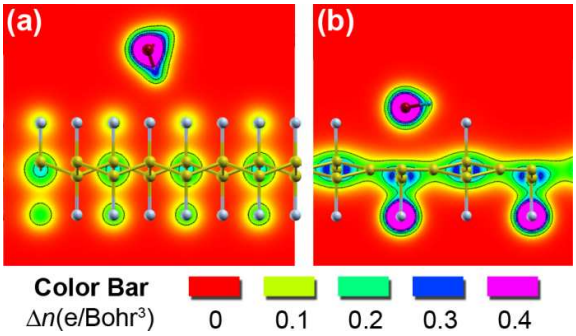

Figure 6. The charge density contour of most energetically favorable structures of a water molecule absorbed on (a) CF (No. 1) and (b) C_4F (No. 24).

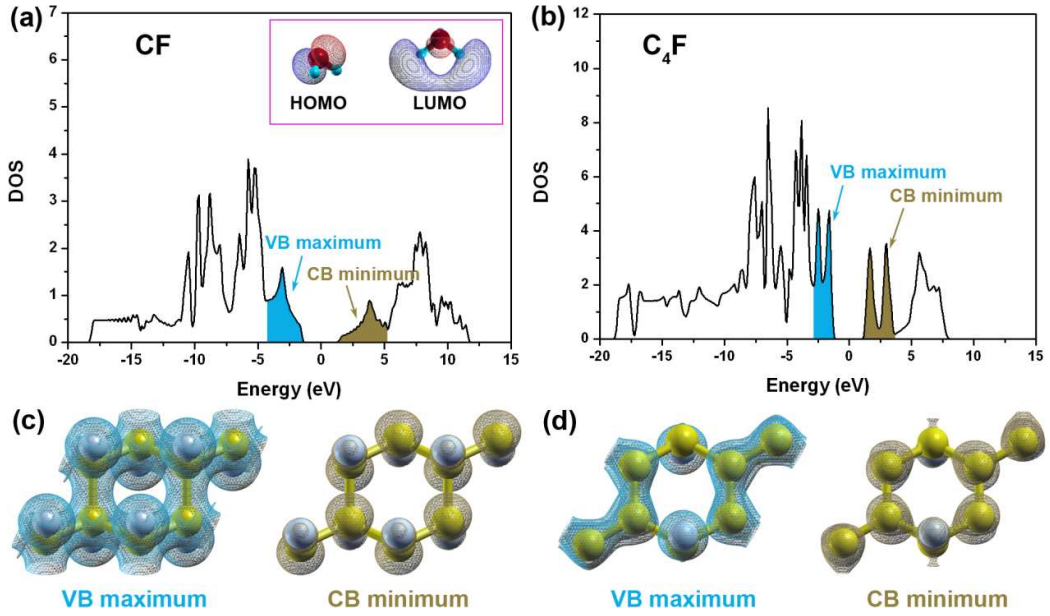

Figure 7. The VB maximum and CB minimum are shadowed in the DOS plots of (a) CF and (b) C_4F. Inset to (a) are the HOMO and the lowest unoccupied molecular orbitals (LUMO) of a water molecule. Visualization of the VB maximum and CB minimum of (c) CF and (d) C_4F by integrated local density of states. The iso-value is 0.015.

B. Transition from hydrophobicity to superhydrophilicity

The GGA method is known to underestimate the nonlocal forces, which gives a lower bound of the adsorption energy.[23, 24] On the other hand, the upper bound can be obtained by employing the LDA method which overestimates these interactions.[11, 23] By considering both the lower and upper bounds, the hydrophilic/hydrophobic nature of the fluorinated graphene surfaces can be captured.

The GGA method with Perdew-Burke-Ernzerhof (GGA-PBE) parameterization[25] predicted the adsorption energies of the representative configurations to be -30 meV (No. 1 for CF), -95 meV (No. 20 for C_4F) and -184 meV (No. 24 for C_4F). These interactions are substantially lower than the corresponding values predicted by the

LDA method. The inter distances by GGA-PBE are enlarged by more than 20%,[12] substantially lowering the Coulomb attraction at a distance of 2 – 3 Å. Meanwhile, the method itself underestimates the Coulomb interaction by ~ 13% for the inadequate description of the attraction.[26]

It is noted that the adsorption energy bound (-30 meV ~ -117 meV) for H_2O/CF is smaller than that of the H_2O/graphene system, as predicted to be -47 meV (lower bound) and -151 meV (upper bound) by GGA[23] and LDA[22], respectively. This observation suggests that the CF surface is more hydrophobic than graphene (CA ~ 92°), which is consistent with the larger CA of CF (~123°) in a recent experimental study.[7] For the H_2O/C_4F system, the adhesion energy (γ_a) was estimated in the range of 213 ~ 660 mJ/m^2, based on the adsorption energies calculated by LDA and GGA methods (Figure S2). The contact angle (θ_c) can thus be deduced from the Young's equation $\cos\theta_c = (\gamma_a - \gamma_w) / \gamma_w$, where γ_w = 72 mJ/m^2 is the surface energy of water. For both lower and upper bounds, the right-hand side of the Young's equation is larger than one, leading to a zero contact angle in physics and rendering a superhydrophilic surface of C_4F. The wetting behaviors of CF and C_4F shows a transition from hydrophobicity to superhydrophilicity.

C. Mechanism of the high adsorption energy

Adsorption energy is contributed by the *van der* Waals, electrostatics and induction interactions. The electrostatic attraction can be calculated by the Coulomb's law by considering the distributed charge density from DFT. Due to the large difference in electronegativity values of C (2.55) and F (3.98), the high polarity of the

C-F bond leads to charge localization. Projected DOS analysis shows a net charge of 0.232 e transferred from the sp^3 C atom to the nearest F atom. There is no charge transfer between two neighboring C atoms. All sp^2 C atoms are neutral. Figure 8a depicts the net charge distribution of H_2O/C_4F. For the water molecule, the net charges are –0.830 e and 0.415 e for the O and H atoms, respectively.[27, 28] These values are widely used in molecular dynamics simulations to reproduce the electrostatic potential of water molecules with force field models, such as TIP3P. As a first-order approximation, the electrostatic potential energy (E_C) can be calculated as $E_C = q_1 q_2 / 4\pi\varepsilon_0 r$, where ε_0 represents the permittivity of free space, q_1 and q_2 are the net charges in H_2O and FG, respectively, with a relative distance of r. Figure 8b plots the coulomb energies of various optimized configurations, contributing a large portion of the adsorption energy in C_4F. Only mitigated London dispersion forces are present for fluorinated graphenes due to the high electronegativity of fluorine, as frequently observed in fluorocarbons.[1] The coulomb energy is in the range of –161 meV ~ –315 meV for the H_2O/C_4F system. Therefore, it is not surprising to observe the high adsorption energy of H_2O/C_4F, in sharp contrast to H_2O/CF.

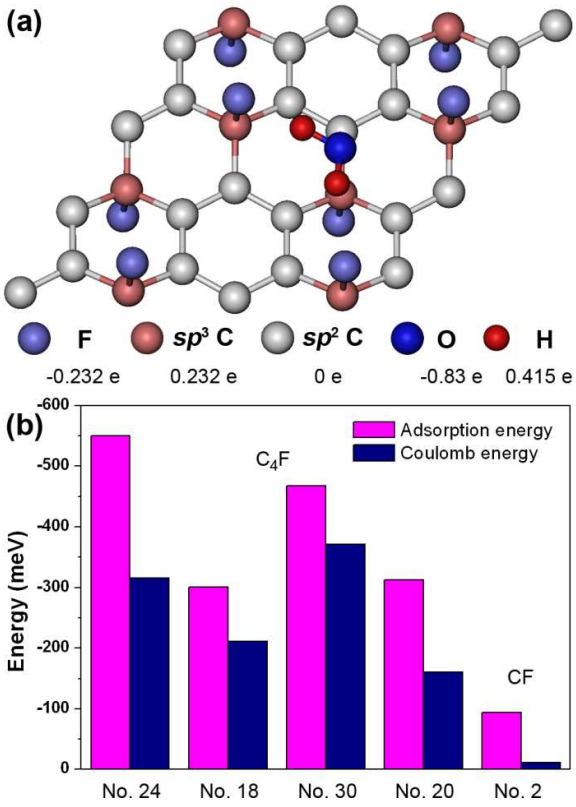

Figure 8. (a) Schematics of coulomb field model. The negatively and positively charged atoms are colored in blue and red, respectively. (b) The adsorption energies and coulomb energies for various energetically favorable configurations.

Conclusions

Two fluorocarbon derivatives of graphene, CF and C_4F, have similar structures and electronic properties, but show profound difference in water's adsorption energies. The enhanced orbital hybridization and the large Coulomb attraction both contribute to the high water adsorption energy on C_4F. The VB maximum and CB minimum of C_4F are mainly located on the sp^2-hybridized C atoms. The O atom in water molecules can be closely aligned with the C atoms, leading to the maximization of the hybridization. However, the CB minimum of CF cannot be approached by O atom,

resulting in a large separation between the O atom and the C atoms. The dominant interaction is among the H and F atoms. The high adsorption energy (-550 meV) of C_4F is also contributed by the Coulomb attraction among the non-bonding interactions. This is consistent with our proposed model that gives a coulomb energy of ~ -315 meV for the H_2O/C_4F system. The above observations suggest the possibilities to replace CF with C_4F in electronic devices, shedding light on a new route to resolve the key difficulty in surface chemical inertness.

Acknowledgments

H Wang acknowledges the financial support from the National Natural Science Foundation of China (Grant No. 11322219), National Program for Special Support of Top-Notch Young Professionals and Fundamental Research Funds for the Central Universities (2014XZZX003). The computational work carried out by TianHe-1(A) system at National Supercomputer Center in Tianjin is gratefully acknowledged.

References

1. R. R. Nair, W. Ren, R. Jalil, I. Riaz, V. G. Kravets, L. Britnell, P. Blake, F. Schedin, A. S. Mayorov, S. Yuan, M. I. Katsnelson, H.-M. Cheng, W. Strupinski, L. G. Bulusheva, A. V. Okotrub, I. V. Grigorieva, A. N. Grigorenko, K. S. Novoselov and A. K. Geim, *Small*, 2010, **6**, 2877-2884.

2. K.-J. Jeon, Z. Lee, E. Pollak, L. Moreschini, A. Bostwick, C.-M. Park, R. Mendelsberg, V. Radmilovic, R. Kostecki, T. J. Richardson and E. Rotenberg, *Acs Nano*, 2011, **5**, 1042-1046.

3. S. Kwon, J.-H. Ko, K.-J. Jeon, Y.-H. Kim and J. Y. Park, *Nano Letters*, 2012, **12**, 6043-6048.

4. R. Stine, W.-K. Lee, K. E. Whitener, Jr., J. T. Robinson and P. E. Sheehan, *Nano letters*, 2013, **13**, 4311-4316.

5. M. A. Ribas, A. K. Singh, P. B. Sorokin and B. I. Yakobson, *Nano Research*, 2011, **4**, 143-152.

6. J. T. Robinson, J. S. Burgess, C. E. Junkermeier, S. C. Badescu, T. L. Reinecke, F. K. Perkins, M. K. Zalalutdniov, J. W. Baldwin, J. C. Culbertson, P. E. Sheehan and E. S. Snow, *Nano Letters*, 2010, **10**, 3001-3005.

7. M. Zhang, Y. C. Ma, Y. Y. Zhu, J. F. Che and Y. H. Xiao, *Carbon*, 2013, **63**, 149-156.

8. D. B. Farmer and R. G. Gordon, *Nano Letters*, 2006, **6**, 699-703.

9. J. M. P. Alaboson, Q. H. Wang, J. D. Emery, A. L. Lipson, M. J. Bedzyk, J. W. Elam, M. J. Pellin and M. C. Hersam, *Acs Nano*, 2011, **5**, 5223-5232.

10. B. Lee, S.-Y. Park, H.-C. Kim, K. Cho, E. M. Vogel, M. J. Kim, R. M. Wallace and J. Kim, *Applied Physics Letters*, 2008, **92**, 203102.

11. M. Vanin, J. J. Mortensen, A. K. Kelkkanen, J. M. Garcia-Lastra, K. S. Thygesen and K. W. Jacobsen, *Physical Review B*, 2010, **81**, 081408.

12. T. Björkman, A. Gulans, A. V. Krasheninnikov and R. M. Nieminen, *Journal of Physics: Condensed Matter*, 2012, **24**, 424218.

13. T. Gould, S. Lebegue and J. F. Dobson, *Journal of Physics-Condensed Matter*, 2013, **25**, 445010.

14. I. Hamada and M. Otani, *Physical Review B*, 2010, **82**, 153412.

15. G. Paolo, B. Stefano, B. Nicola, C. Matteo, C. Roberto, C. Carlo, C. Davide, L. C. Guido, C. Matteo, D. Ismaila, C. Andrea Dal, G. Stefano de, F. Stefano, F. Guido, G.

Ralph, G. Uwe, G. Christos, K. Anton, L. Michele, M.-S. Layla, M. Nicola, M. Francesco, M. Riccardo, P. Stefano, P. Alfredo, P. Lorenzo, S. Carlo, S. Sandro, S. Gabriele, P. S. Ari, S. Alexander, U. Paolo and M. W. Renata, *J. Phys-Condens. Mat.*, 2009, **21**, 395502.

16. A. M. Rappe, K. M. Rabe, E. Kaxiras and J. D. Joannopoulos, *Phys. Rev. B*, 1990, **41**, 1227-1230.

17. H. J. Monkhorst and J. D. Pack, *Phys. Rev. B*, 1976, **13**, 5188-5192.

18. F. Karlicky, K. Kumara Ramanatha Datta, M. Otyepka and R. Zboril, *ACS nano*, 2013, **7**, 6434-6464.

19. A. Vyalikh, L. G. Bulusheva, G. N. Chekhova, D. V. Pinakov, A. V. Okotrub and U. Scheler, *Journal of Physical Chemistry C*, 2013, **117**, 7940-7948.

20. H. Sahin, M. Topsakal and S. Ciraci, *Physical Review B*, 2011, **83**, 115432.

21. C.-H. Hu, P. Zhang, H.-Y. Liu, S.-Q. Wu, Y. Yang and Z.-Z. Zhu, *Journal of Physical Chemistry C*, 2013, **117**, 3572-3579.

22. J. Ma, A. Michaelides, D. Alfè, L. Schimka, G. Kresse and E. Wang, *Physical Review B*, 2011, **84**, 033402.

23. O. Leenaerts, B. Partoens and F. M. Peeters, *Physical Review B*, 2008, **77**, 125416.

24. O. Leenaerts, B. Partoens and F. M. Peeters, *Physical Review B*, 2009, **79**, 235440.

25. J. P. Perdew, K. Burke and M. Ernzerhof, *Phys. Rev. Lett.*, 1996, **77**, 3865-3868.

26. J. Klimes and A. Michaelides, *The Journal of Chemical Physics*, 2012, **137**, 120901-120912.

27. G. Hummer, J. C. Rasaiah and J. P. Noworyta, *Nature*, 2001, **414**, 188-190.

28. H. L. Liu and G. X. Cao, *Journal of Physical Chemistry C*, 2013, **117**, 4245-4252.